# Effect of temperature on the tuning of a piezoelectric resonant shunt composed of variable inductance or variable capacitance

Robin Darleux, Boris Lossouarn, Jean-François Deü

# Effect of temperature on the tuning of a piezoelectric resonant shunt composed of variable inductance or variable capacitance

**R. Darleux** [1], **B. Lossouarn** [1], **J.-F. Deü** [1]
[1] Laboratoire de Mécanique des Structures et des Systèmes Couplés (LMSSC),
Conservatoire national des arts et métiers (Cnam),
292 rue Saint-Martin, 75003 Paris, France
e-mail: **robin.darleux@lecnam.net**

## Abstract
The piezoelectric resonant shunt is an electromechanical device that can significantly damp mechanical vibrations if it is finely tuned. However, temperature may influence the electrical components of the shunt and the mechanical parameters of the vibrating structure, and deteriorate the damping performance as a consequence. The objective of this work is to describe how inductive and capacitive components can be chosen so that the shunt tuning is maintained in the case of temperature variations. Two solutions of fully passive adaptive shunts are developed, tested and compared. The first solution includes a variable inductance. In contrast, the second solution includes a variable capacitance and intends on keeping the shunt inductance as constant as possible. Experiments validate the concept of a resonant shunt that autonomously adapts to temperature variations.

## 1 Introduction

Mechanical vibrations can be mitigated by bonding piezoelectric patches on the surface of a vibrating structure, as it allows transferring part of the vibration energy to an electrical circuit where it can be dissipated in a resistive component. A well documented electrical circuit is the resonant shunt [1], which is the electromechanical equivalent of a tuned mass damper (also called dynamic vibration absorber). The vibration damping induced by this device is mainly owed to a precise tuning of the electrical parameters [2, 3, 4]. Besides, electrical parameters and mechanical characteristics of the system may strongly evolve with environmental parameters such as temperature. Several studies have highlighted the dependence in temperature of piezoelectric properties [5, 6]. While solutions have been proposed for an online tuning of the resonant shunt, they are either limited to a few decibels of vibration damping [7], or active solutions that require external power [8]. Recently, the choice of the magnetic material of the considered inductor has been highlighted as a way to passively counterbalance the tuning variations of a resonant shunt [9].

The objective of this work is to validate the concept of an autonomous resonant shunt, whose tuning is maintained in case of temperature variations. To do so, an electromechanical model of the structure is developed in section 2. Two solutions, denoted solutions A and B, are proposed: the adapting component is a variable inductance in the solution A, while it is a variable capacitance in the solution B. Then in section 3, we describe the experimental setup of a vibrating cantilever beam covered with a pair of piezoelectric patches. From there, the design of electrical components for both solutions is performed. Finally, experimental results in section 4 show that both solutions sustain the tuning up to at least $50\,^{\circ}\mathrm{C}$. In the end, the concept of a reliable and fully passive resonant shunt adpating to temperature variations is validated.

| Mechanical quantity | | Electrical quantity |
|---|---|---|
| Force | $\leftrightarrow$ | Voltage |
| Velocity | $\leftrightarrow$ | Electrical current |
| Compliance | $\leftrightarrow$ | Capacitance |
| Mass | $\leftrightarrow$ | Inductance |
| Viscous damping | $\leftrightarrow$ | Resistance |

Table 1: Direct electromechanical analogy

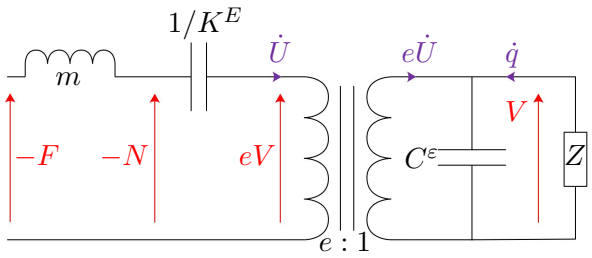


Figure 1: Equivalent electrical circuit of the shunted structure

## 2 Electromechanical model of a piezoelectric resonant shunt

### 2.1 Piezoelectric shunt damping

Piezoelectric shunt damping consists in bonding a vibrating structure with piezoelectric transducers, and connecting them to an electrical circuit. The electrical energy transferred to this circuit is dissipated in a resistive component, and mechanical vibrations are mitigated as a consequence. In this article, we consider the case of two piezoelectric patches covering opposite faces of a cantilever beam. Three stages are needed to describe the dynamics of the system: developing an electromechanical model of the piezoelectric transducer, developing a mechanical model of the structure, and defining the shunt components.

We propose a one-dimensional model of a piezoelectric transducer:

$$\begin{aligned} N &= K^E U - eV, \\ q &= C^\varepsilon V + eU, \end{aligned} \tag{1}$$

where $N$ is the normal force applied to the transducer, $q$ is the electric charge on an electrode, $U$ is the displacement in the longitudinal direction, and $V$ is the voltage between the electrodes of the piezoelectric device. The constants $e$, $K^E$ and $C^\varepsilon$ are the coupling coefficient, the structural stiffness when the piezoelectric transducer is short-circuited (i.e. when $V = 0$), and the piezoelectric capacitance under no displacement (i.e. when $U = 0$), respectively. The mechanical structure is then modeled as an undamped one degree-of-freedom system, whose dynamics can be expressed by

$$m\ddot{U} + K^D U = F + \frac{e}{C^\varepsilon} q, \tag{2}$$

where $m$ is the mass, $F$ is the excitation force, and $K^D = K^E + e^2/C^\varepsilon$ is the stiffness in open-circuit. Equation (2) highlights the equivalent mechanical quantities on its left side, and the external forces applied to the structure on its right side. Finally, the structure is shunted with an impedance $Z$. Ohm's law applied to the shunt impedance gives

$$V = -Z\dot{q}. \tag{3}$$

The use of a direct electromechanical analogy, summed up in Table 1, allows to define the equivalent electrical circuit of the electromechanical system based on equations (1), (2) and (3). It is represented in Figure 1. These equations can also be combined to obtain the dimensionless transfer function between the displacement and the excitation at angular frequency $\Omega$:

$$\frac{U}{F/K^D} = \frac{1 + \mathrm{j}\Omega C^\varepsilon Z}{\left[1 - \left(\frac{\Omega}{\Omega_\mathrm{O}}\right)^2\right](1 + \mathrm{j}\Omega C^\varepsilon Z) - \frac{k_{c0}^2}{1+k_{c0}^2}}, \tag{4}$$

with $\mathrm{j}^2 = -1$. In this last equation, $k_{c0}$ is the coupling factor, and $\Omega_\mathrm{O}$ and $\Omega_\mathrm{S}$ are the mechanical resonance angular frequencies in open-circuit (i.e. when $q = 0$) and in short-circuit (i.e. when $V = 0$), respectively. These quantities are defined by

$$\Omega_\mathrm{O} = \sqrt{\frac{K^D}{m}}, \qquad \Omega_\mathrm{S} = \sqrt{\frac{K^E}{m}}, \qquad k_{c0} = \sqrt{\frac{\Omega_\mathrm{O}^2 - \Omega_\mathrm{S}^2}{\Omega_\mathrm{S}^2}}. \tag{5}$$

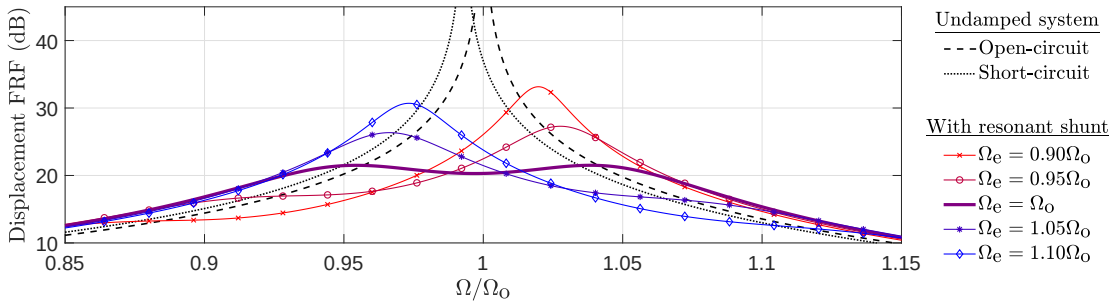


Figure 2: Displacement FRF around the resonance for $k_{c0} = 0.12$ and $\xi_e = (\xi_e)_{opt}$

## 2.2 Adaptive tuning of a resonant shunt in case of temperature variations

### 2.2.1 Solution A: Resonant shunt with variable inductance

A basic resonant shunt is first considered. The impedance $Z$ consists of a resistance $R$ and an inductance $L$ connected in series:

$$Z = R + \mathrm{j}\Omega L. \tag{6}$$

The transfer function in equation (4) then becomes

$$\frac{U}{F/K^D} = \frac{1 + 2\mathrm{j}\frac{\xi_e}{\Omega_e}\Omega - \left(\frac{\Omega}{\Omega_e}\right)^2}{\left[1 - \left(\frac{\Omega}{\Omega_O}\right)^2\right]\left[1 + 2\mathrm{j}\frac{\xi_e}{\Omega_e}\Omega - \left(\frac{\Omega}{\Omega_e}\right)^2\right] - \frac{k_{c0}^2}{1+k_{c0}^2}}, \tag{7}$$

with $\Omega_e$ the electrical resonance angular frequency and $\xi_e$ the electrical damping defined by

$$\Omega_e = \frac{1}{\sqrt{LC^\varepsilon}}, \qquad \xi_e = \frac{R}{2}\sqrt{\frac{C^\varepsilon}{L}}. \tag{8}$$

The main drawback of the resonant shunt is the need for a precise tuning [2, 3, 4]. The transfer function criterion detailed in [2] states that the optimal values of these electrical parameters are:

$$(\Omega_e)_{opt} = \Omega_O, \qquad (\xi_e)_{opt} = \sqrt{\frac{3}{8}}k_{c0}. \tag{9}$$

The frequency response function (FRF) in equation (7) is represented in Figure 2. Variations of the electric damping $\xi_e$ are not considered since it has little influence on the vibration mitigation when compared to $\Omega_e$ variations [2, 3, 4]. Figure 2 shows that the damping performance drops as soon as the electrical resonance differs from its optimal value: for $k_{c0} = 0.12$, a difference of 10 % between $\Omega_e$ and its optimal value adds nearly 10 dB to the transfer function peak. Hence, the tuning condition in equation (9) should be verified in any situation to maintain the vibration damping. However, mechanical and electrical parameters of the system may vary when temperature changes. If the evolutions with temperature of the mechanical resonance and the piezoelectric capacitance are given data, then the inductance is the control parameter. That means the value of $L$ should be adapted so that it always verifies

$$\Omega_O^2(T) = \frac{1}{L(T)\,C^\varepsilon(T)}. \tag{10}$$

In this work, we suppose that $\Omega_O$, $C^\varepsilon$ and $L$ evolve linearly over the considered temperature range, and the associated temperature coefficients are noted $\alpha_{\Omega_O}$, $\alpha_{C^\varepsilon}$ and $\alpha_L$, respectively. Room temperature is noted $T_0$.

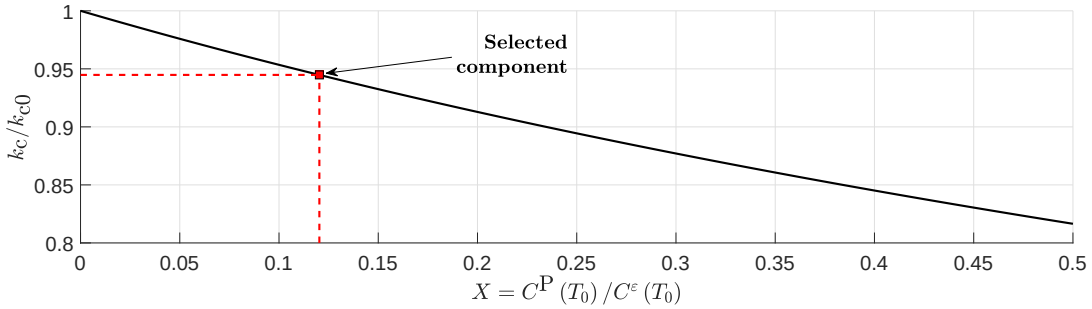


Figure 3: Evolution of the coupling coefficient in case of an added parallel capacitance

The evolutions with temperature of these quantities can be written as follows:

$$\begin{aligned} \Omega_O(T) &= \Omega_O(T_0)\left[1+\alpha_{\Omega_O}(T-T_0)\right], \\ C^\varepsilon(T) &= C^\varepsilon(T_0)\left[1+\alpha_{C^\varepsilon}(T-T_0)\right], \\ L(T) &= L(T_0)\left[1+\alpha_L(T-T_0)\right]. \end{aligned} \tag{11}$$

A linear approximation of equation (10) gives the relation between the temperature coefficients that should be verified to keep the resonant shunt tuned:

$$\alpha_L = -\left(2\alpha_{\Omega_O} + \alpha_{C^\varepsilon}\right). \tag{12}$$

This solution for a passive temperature adjustment of the resonant shunt tuning, denoted solution A, requires to design the inductor according to temperature characteristics of the system. A limit of this solution would be that the inductance of the passive inductors may depend on the electrical current, as Legg reported in [10]. Since the electrical current in the shunt is generated by mechanical vibrations, the shunt inductance may strongly depend on the amplitude of the mechanical excitation. Furthermore, the temperature and electrical current characteristics of these inductors are interdependent, because they both depend on the magnetic circuit properties. As a consequence, designing inductors with large variations of inductance with temperature may lead to large variations with the excitation amplitude as well. For this reason, another solution is developed below.

### 2.2.2 Solution B: Resonant shunt with additional variable capacitance

For this second proposed solution, the objective is first to design an inductor that is as stable as possible with respect to temperature and electrical current. Then, a capacitance $C^P$ is added in parallel with a series $RL$ shunt. This added capacitance should be designed to maintain the damping performance when temperature evolves. In this case, the impedance $Z$ is

$$Z = \frac{R + \mathrm{j}\Omega L}{1 + \mathrm{j}\Omega R C^P - L C^P \Omega^2}. \tag{13}$$

The system FRF is still expressed by equation (7). The only differences are that the piezoelectric capacitance $C^\varepsilon$ is replaced by $C^\varepsilon + C^P$, and that the coupling factor $k_{c0}$ is replaced by a lower coupling factor $k_c$. Indeed, using the parameters defined in (5) allows to express the equivalent coupling coefficient $k_c$:

$$\frac{k_c}{k_{c0}} = \frac{1}{\sqrt{1+\frac{C^P}{C^\varepsilon}}}. \tag{14}$$

The evolution of the coupling coefficient with the additional capacitance is represented in Figure 3. It shows that adding some capacitance to the shunt deteriorates the electromechanical coupling, and thus the damping

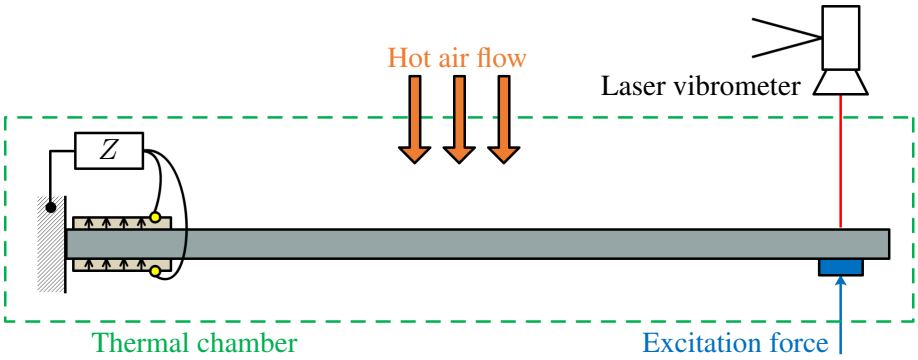


Figure 4: Sketch of the experimental setup inside the thermal chamber

performance [2, 11]. In this situation, the tuning condition derived from equation (10) becomes

$$\Omega_{\mathrm{O}}^2(T) = \frac{1}{L(T)\left[C^{\varepsilon}(T) + C^{\mathrm{P}}(T)\right]}. \tag{15}$$

If the evolutions with temperature of the mechanical resonance, the piezoelectric capacitance and the inductance are given data, then the control parameters are the added capacitance and its temperature characteristics. We assume that $C^{\mathrm{P}}$ evolves linearly over the considered temperature range, which means $C^{\mathrm{P}}(T) = C^{\mathrm{P}}(T_0)\left[1 + \alpha_{C^{\mathrm{P}}}(T - T_0)\right]$ with $\alpha_{C^{\mathrm{P}}}$ its temperature coefficient. A linear approximation of equation (15) shows that the tuning condition becomes

$$\alpha_{C^{\mathrm{P}}} = -\left[\left(\alpha_L + 2\alpha_{\Omega_{\mathrm{O}}} + \alpha_{C^{\varepsilon}}\right)\frac{C^{\varepsilon}(T_0)}{C^{\mathrm{P}}(T_0)} + \alpha_L + 2\alpha_{\Omega_{\mathrm{O}}}\right]. \tag{16}$$

Using dimensionless quantities, the tuning condition can also be written:

$$Y = -\left(\frac{a}{X} + b\right), \qquad \text{with} \quad Y = \frac{\alpha_{C^{\mathrm{P}}}}{\alpha_{C^{\varepsilon}}}, \quad X = \frac{C^{\mathrm{P}}(T_0)}{C^{\varepsilon}(T_0)}, \quad b = \frac{\alpha_L + 2\alpha_{\Omega_{\mathrm{O}}}}{\alpha_{C^{\varepsilon}}}, \quad a = b + 1. \tag{17}$$

This solution for a passive temperature adaptation of the resonant shunt is denoted solution B. Solution B may offer a more stable solution than solution A. Indeed, the electrical current should have little influence on the inductance, since it has been designed to this end. However, more stability is achieved at the expense of the damping performance. For this reason, the added capacitance should be as small as possible.

# 3 Design of electrical components

## 3.1 Experimental setup

The experimental setup consists of a cantilever beam covered with two piezoelectric patches close to the clamped end. The duralumin beam is 170 mm long, 25 mm large and 2 mm thick. The PIC 151 PZT patches are 25 mm long, 20 mm large and 0.5 mm thick. The excitation and the velocity measurement are both made at the free end of the beam. The setup is eventually heated with a heat gun inside a thermal chamber, in which measurements are made with an infrared thermometer in steady thermal state. A sketch of the setup is represented in Figure 4.

The evolutions with temperature of the mechanical resonance $\Omega_{\mathrm{O}}$ and of the piezoelectric capacitance $C^{\varepsilon}$ are plotted in Figure 5. The estimated temperature coefficients are $\alpha_{\Omega_{\mathrm{O}}} = -0.5 \cdot 10^{-3}\mathrm{K}^{-1}$ and $\alpha_{C^{\varepsilon}} = 3.1{\cdot}10^{-3}\mathrm{K}^{-1}$. The evolution with temperature of the piezoelectric capacitance is in rough agreement with the manufacturer data. The main reason for the remaining difference is the variations of the structural properties, as it leads to piezoelectric capacitance variations because of the electromechanical coupling.

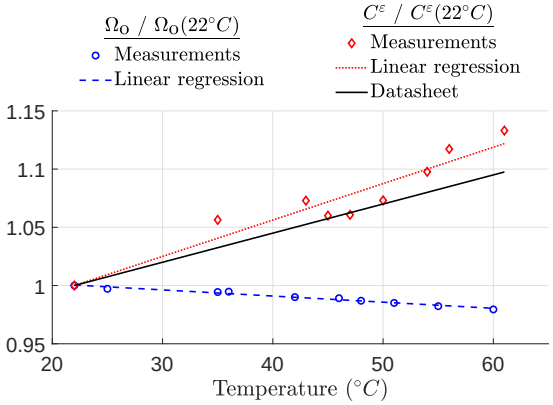


Figure 5: Evolution with temperature of the piezoelectric capacitance and the mechanical resonance angular frequency in open-circuit divided by their respective values at room temperature

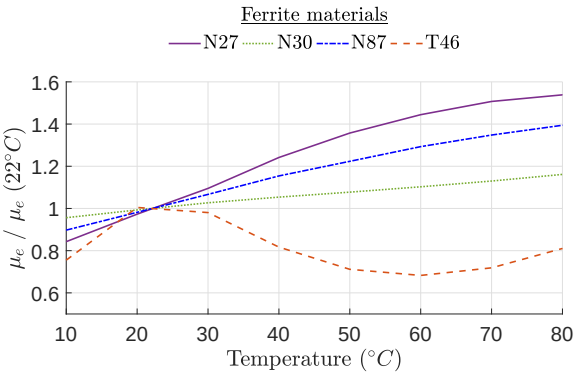


Figure 6: Effective permeability evolution with temperature of available ferrite materials in ungapped E 16/8/5 core geometry, extracted from datasheets

## 3.2 Variable inductor for solution A

Optimized inductors for piezoelectric shunt damping usually require large inductance and small resistance values. Passive inductors meeting these requirements can be made following the method described in [12]. Inductors are produced by winding $N$ turns of conductive wire around magnetic cores of effective permeability $\mu_e$. This permeability depends on the properties of the magnetic circuit [13]. The obtained inductance value is proportionnal to $N^2$ and $\mu_e$, with a geometry depending constant $\beta$:

$$L = \beta \mu_e N^2. \tag{18}$$

Equation (12) shows the inductance has to vary with temperature to keep the resonant shunt tuned. Since $\beta$ and $N$ do not depend on temperature, equation (18) shows the temperature coefficient of the effective permeability $\alpha_{\mu_e}$ is equal to $\alpha_L$. For practical reasons related to ferrite materials availability, the ungapped E 16/8/5 core geometry from core manufacturer Epcos TDK has been selected. The temperature characteristics of several available ferrite materials are compared in Figure 6. According to equation (12) and measurements in subsection 3.1, designing a resonant shunt adapting to temperature variations requires an inductor whose inductance decreases when temperature rises. In an other work [9], we have shown that the T46 ferrite material is the one that should be selected among the available ones.

We measure that $C^\varepsilon = 38.3$ nF and $\Omega_O/2\pi = 322$ Hz, so the required inductance is estimated at $L = 6.38$ H using equation (10). Since data from manufacturers give $\beta = 0.672$ nH and $\mu_e = 1410$, we calculate $N = 2600$ turns using equation (18). The produced inductor is then tested with an LCR-meter at 322 Hz. Inductance variations with temperature and electrical current are plotted in Figure 7. When available, data from manufacturers are represented as well.

In Figure 7(a), the available datasheet do not accurately predict the inductance evolution from 22 °C to 60 °C. Moreover, the predicted decrease of the inductance is only obtained at low levels of excitation and below 42 °C. In Figure 7(b), our measurements show as well a decrease of the inductance under 40 µA and 42 °C. However, as soon as the environmental parameters are outside this range of low temperature and low levels of excitation, the inductance increases. In hindsight, this practical characterization highlights the correlation that can exist between temperature and excitation effects on the inductance. For this reason, it can be difficult to design an inductor whose characteristics meet our requirements over a wide range of both temperature and excitation amplitude. This is the reason why the solution B has been developed.

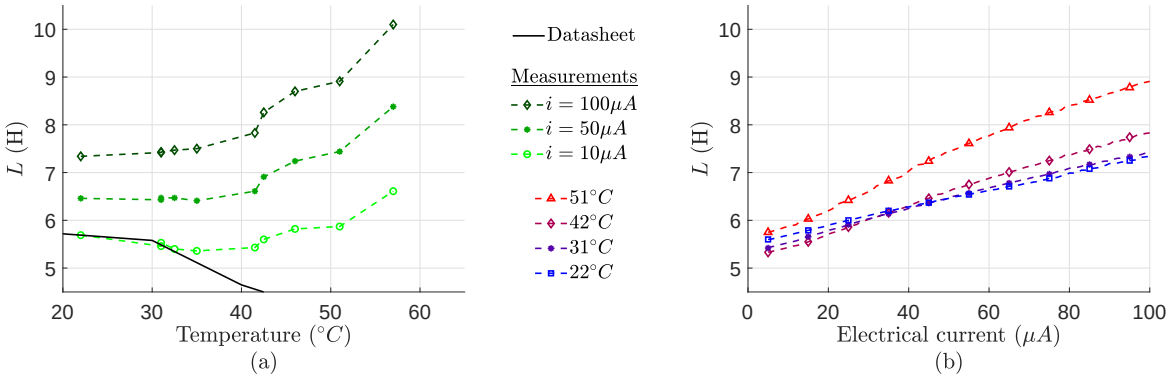


Figure 7: Effect of (a) temperature and (b) electrical current on the T46 ferrite-based inductor.

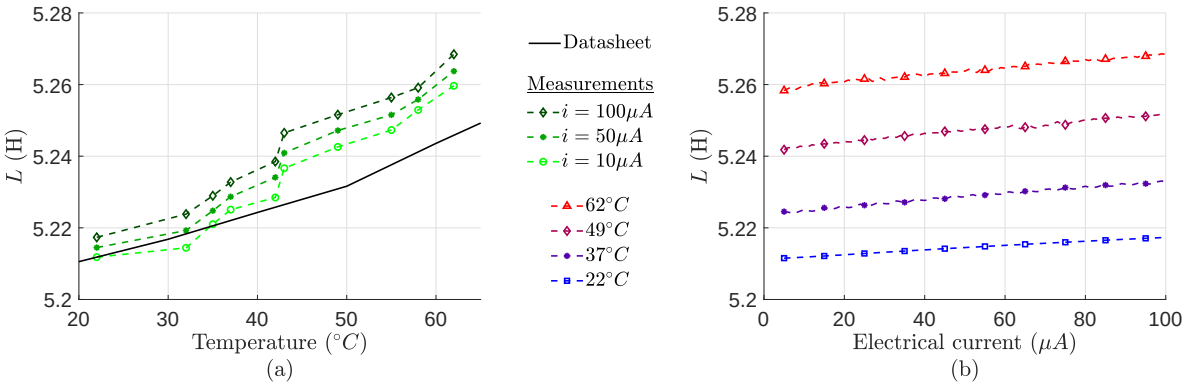


Figure 8: Effect of (a) temperature and (b) electrical current on the N48 ferrite-based inductor. Notice the scale of the y-axis.

## 3.3 Variable capacitor for solution B

In the case of solution B, the objective is first to design an inductor whose variations with electrical current and temperature are as small as possible. Equation (18) is still considered. Obtaining the required inductance value while minimizing $\alpha_{\mu_e}$ is possible by adding an air gap in the magnetic circuit of the component [13]. The N48 ferrite material with the gapped RM10 core geometry from Epcos TDK has been selected. In this case, $\beta = 2.48$ nH, $\mu_e = 254$ and $N = 2870$ turns.

Figure 8 shows the characteristic of the produced inductor. Data from core manufacturers do not precisely predict the inductance evolution with temperature, which may be due to a smaller air gap than anticipated. The estimated temperature coefficient for $L$ is $(\alpha_L)_{\mathrm{B}} = 2.5 \cdot 10^{-4}\mathrm{K}^{-1}$. This value is nearly thirty times smaller than $(\alpha_L)_{\mathrm{A}}$ from subsection 3.2. Moreover, electrical current and temperature effects do not seem strongly correlated. Hence, the produced inductor meet our requirements by having a nearly constant inductance when environmental parameters evolve.

The next step is to select the added capacitance $C^{\mathrm{P}}$. Given the decrease of $k_{\mathrm{c}}$ expressed in equation (14) and plotted in Figure 3, the goal is to add the smallest possible value of $C^{\mathrm{P}}$. Figure 9 represents the optimal tuning possibilities for solution B, as expressed in equation (17). Values of $\alpha_{\Omega_{\mathrm{o}}}$ and $\alpha_{C^{\varepsilon}}$ are estimated in subsection 3.1. The graph shows that the smaller $C^{\mathrm{P}}$ is, the bigger its variations have to be to maintain the tuning. As a consequence, we selected ceramic capacitors of class 2 [14], which are characterized by large variations of capacitance with temperature over their working range. Characteristics of some of the dielectrics that vary the most with temperature are extracted from datasheets and added to Figure 9. The selected capacitor is a Y5V $4.7\,\mathrm{nF}$ capacitor, as it is the closest component to the optimal curve among the available ones. Its measured characteristics is rougly in agreement with its datasheet. Both are placed

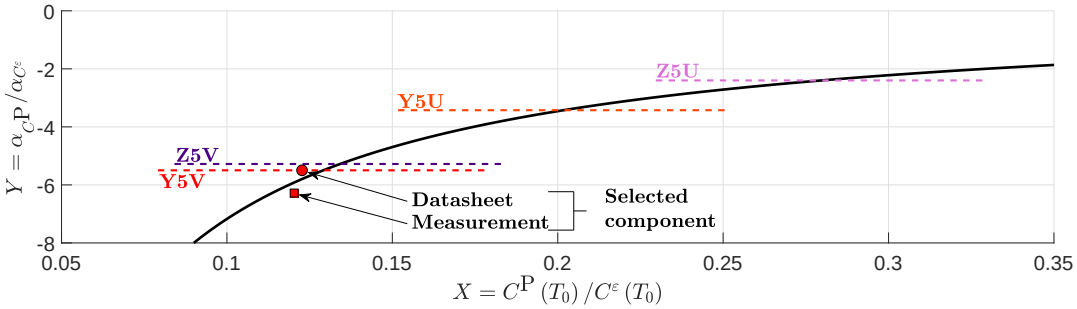


Figure 9: Solid line: Optimal characteristics of the added capacitance. Dashed lines: Usual temperature variations of several class 2 dielectrics. Red points: selected capacitor.

on Figure 9. The selected component is added to Figure 3 as well, and it shows that trading off some of the damping performance for more stability makes sense, since the coupling coefficient $k_{\mathrm{c}}$ is only 6 % lower than $k_{\mathrm{c}0}$.

# 4 Vibration damping of a clamped beam

## 4.1 Adaptive resonant shunt using solution A

The solution A is considered for passive vibration damping of the second bending mode of a clamped beam. The inductance of the resonant shunt is the T46 ferrite-based inductor designed in subsection 3.2. At room temperature, the shunt resistance is intentionally set under its theoretical optimal value [2, 4]. The evolution of the shunt tuning is thus more easily detected. Experiments are conducted at low levels of excitation to benefit from the inductance decrease spotted on Figure 7. The experimental setup is represented in Figure 4.

Experimental FRFs are compared at different temperatures in Figure 10. The shunt tuning is preserved from room temperature to around 51 °C. It appears that the system benefits from a larger decrease of the inductance value than what had been anticipated by looking at Figure 7. Moreover, it is experimentally noticed that the shunt gets mistuned at steady thermal state if the excitation amplitude increases. This is a consequence of the strong mutual dependence between electrical current and temperature effects on the inductance, spotted in Figure 7. For this reason, the solution A might keep the shunt tuned only if the mechanical excitation is stable enough over time. This could be a restrictive condition in some practical applications.

## 4.2 Adaptive resonant shunt using solution B

The solution B is now considered to damp bending vibrations of a clamped beam. The inductance of the resonant shunt is the N48 ferrite-based inductor designed in subsection 3.3. The shunt resistance is also set under its optimal value to spot tuning variations more easily.

Experimental FRFs are compared at different temperatures in Figure 11. The shunt seems to get slightly mistuned from room temperature to 50 °C, before coming back to a better tuning at 62 °C. This can be explained by the nonlinear variations with temperature of the added capacitance. Its variations are more important below 50 °C, which explains the initial mistuning. The reduction of the height between the initial peaks at 304 Hz and 334 Hz and the initial valley at 322 Hz may be explained by the increase of the electrical damping with temperature. Moreover, changing the excitation amplitude at steady thermal state do not get the shunt mistuned as much as with solution A. In the end, the shunt tuning is preserved from room temperature to 62 °C, so these results are promising. The electromechanical coupling is reduced when compared to solution A, which leads to a slightly lower damping performance, but stability over a wider range of temperature is achieved.

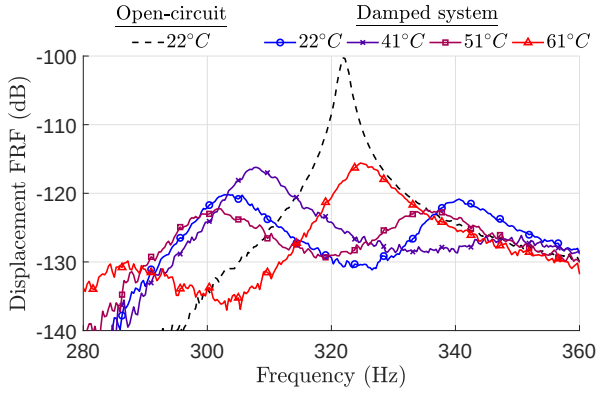


Figure 10: Experimental displacement FRFs at different temperatures with solution A

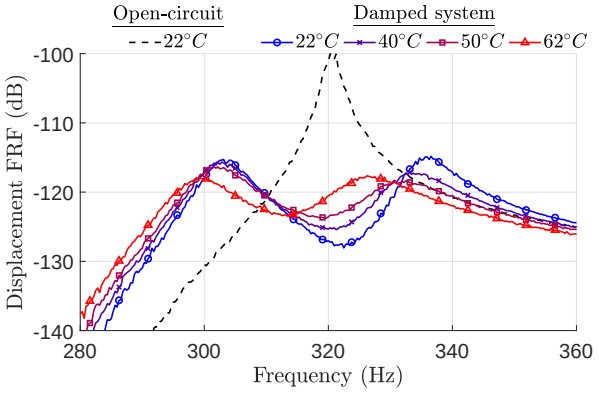


Figure 11: Experimental displacement FRFs at different temperatures with solution B

## 5 Conclusions

The objective of this work is to design a piezoelectric resonant shunt that passively adapts to temperature variations. Two solutions are developed: the first one (denoted solution A) involves a variable inductance, while the second one (denoted solution B) keeps the shunt inductance constant and uses a variable parallel capacitance. An electromechanical model of the vibrating structure connected to the resonant shunt leads to a tuning criterion for each solution. Electrical components are then designed to meet these criteria by taking into account temperature characteristics of the system parameters. When it comes to inductors, we produce them with magnetic circuits. The evolution with temperature of such components depends on the geometry and the material of the magnetic circuit. When it comes to the added parallel capacitance, the class 2 capacitors are selected since they are the ones that vary the most with temperature. All these components are tested, and then used to damp bending vibrations of a cantilever beam. Experimental results show that the shunt tuning is vaguely maintained from room temperature to around 50 °C for solution A, and more precisely maintained from room temperature to more than 60 °C for solution B.

The design of a fully passive and adaptive resonant shunt over a wider range of temperature would require predictive models of electrical components evolutions with temperature. For this matter, solution A would be quite complex to implement, because of the mutual dependence of electrical current and temperature characteristics of the produced inductors. Solution B seems easier to design and implement, but this more predictable and stable solution comes at the expense of the electromechanical coupling. If the slight induced drop of damping performance is acceptable, then solution B may be recommended.

## References

[1] N. W. Hagood and A. Von Flotow, *Damping of structural vibrations with piezoelectric materials and passive electrical networks*, Journal of Sound and Vibration, Vol. 146, No. 2, Elsevier BV (1991), pp. 243–268.

[2] O. Thomas, J. Ducarne, J.-F. Deü, *Performance of piezoelectric shunts for vibration reduction*, Smart Materials and Structures, Vol. 21, No. 1, IOP Publishing (2012), pp. 015008.

[3] J.-W. Park, J.-H. Han, *Sensitivity analysis of damping performances for passive shunted piezoelectrics*, Aerospace Science and Technology, Vol. 33, No. 1, Elsevier BV (2014), pp. 16–25.

[4] M. Berardengo, A. Cigada, S. Manzoni, M. Vanali, *Vibration Control by Means of Piezoelectric Actuators Shunted with LR Impedances: Performance and Robustness Analysis*, Shock and Vibration, Vol. 2015, Hindawi Limited (2015), pp. 1–30.

[5] M. W. Hooker, *Properties of PZT-based piezoelectric ceramics between -150°C and 250°C*, NASA (1998).

[6] C. Miclea, C. Tanasoiu, L. Amarande, C. F. Miclea, C. Plavitu, M. Cioangher, L. Trupina, C. T. Miclea, C. David, *Effect of temperature on the main piezoelectric parameters of a soft PZT ceramic*, Romanian Journal of Information Science and Technology (2007), Vol. 10, No. 3, pp. 243–250.

[7] D. Niederberger, M. Morari, *An autonomous shunt circuit for vibration damping*, Smart Materials and Structures, Vol. 15, No. 2, IOP Publishing (2006), pp. 359–364.

[8] J. J. Hollkamp, T. F. Starchville, *A Self-Tuning Piezoelectric Vibration Absorber*, Journal of Intelligent Material Systems and Structures, Vol. 5, No. 4, SAGE Publications (1994), pp. 559–566.

[9] R. Darleux, B. Lossouarn, J.-F. Deü, *Passive self-tuning inductor for piezoelectric shunt damping considering temperature variations*, Journal of Sound and Vibration, (Accepted for publication), Elsevier BV (2018).

[10] V. E. Legg, *Magnetic Measurements at Low Flux Densities Using the Alternating Current Bridge*, Bell System Technical Journal, Vol. 15, No. 1, IEEE (1936), pp. 39–62.

[11] A. J. Fleming, S. Behrens, S. O. R. Moheimani, *Reducing the inductance requirements of piezoelectric shunt damping systems*, Smart Materials and Structures, Vol. 12, No. 1, IOP Publishing (2013), pp. 57–64.

[12] B. Lossouarn, M. Aucejo, J.-F. Deü, B. Multon, *Design of inductors with high inductance values for resonant piezoelectric damping*, Sensors and Actuators A: Physical, Vol. 259, Elsevier BV (2017), pp. 68–76.

[13] E. C. Snelling, *Soft ferrites*, 2nd edition, CRC Press (1969).

[14] M. J. Pan, C. A. Randall, *A brief introduction to ceramic capacitors*, IEEE Electrical Insulation Magazine, Vol. 26, No. 3, IEEE (2010), pp. 44–50.